8-11-2015

Does the Stellar Disc Flattening Depend on the Galaxy Type

A. V. Mosenkov
Universiteit Gent; Central Astronomical Observatory of RAS; St Petersburg State University

N. Ya. Sotnikova
St Petersburg State University; Isaac Newton Institute of Chile

V. P. Reshetnikov
St Petersburg State University; Isaac Newton Institute of Chile

D. V. Bizyaev
Apache Point Observatory and New Mexico State University; Moscow State University

Stefan Kautsch
Nova Southeastern University, skautsch@nova.edu

Monthly Notices of the ROYAL ASTRONOMICAL SOCIETY
MNRAS **451,** 2376–2389 (2015) doi:10.1093/mnras/stv1085

Does the stellar disc flattening depend on the galaxy type?

A. V. Mosenkov,[1,2,3★] N. Ya. Sotnikova,[3,4★] V. P. Reshetnikov,[3,4] D. V. Bizyaev[5,6] and S. J. Kautsch[7]

[1]*Sterrenkundig Observatorium, Universiteit Gent, Krijgslaan 281 S9, B-9000 Gent, Belgium*
[2]*Central Astronomical Observatory of RAS, Pulkovskoye chaussee 65, 196140 St-Petersburg, Russia*
[3]*St Petersburg State University, Universitetskij pr. 28, 198504 St Petersburg, Stary Peterhof, Russia*
[4]*Isaac Newton Institute of Chile, St Petersburg Branch*
[5]*Apache Point Observatory and New Mexico State University, Sunspot, NM 88349, USA*
[6]*Sternberg Astronomical Institute, Moscow State University, Universitetskij pr. 13, 119991 Moscow, Russia*
[7]*Nova Southeastern University, Fort Lauderdale, FL 33314, USA*

Accepted 2015 May 12. Received 2015 May 12; in original form 2014 June 24

ABSTRACT

We analyse the dependence of the stellar disc flatness on the galaxy morphological type using 2D decomposition of galaxies from the reliable subsample of the Edge-on Galaxies in SDSS catalogue. Combining these data with the retrieved models of the edge-on galaxies from the Two Micron All Sky Survey and the Spitzer Survey of Stellar Structure in Galaxies catalogue, we make the following conclusions.

(1) The disc relative thickness z_0/h in the near- and mid-infrared passbands correlates weakly with morphological type and does not correlate with the bulge-to-total luminosity ratio B/T in all studied bands.

(2) Applying a 1D photometric profile analysis overestimates the disc thickness in galaxies with large bulges making an illusion of the relationship between the disc flattening and the ratio B/T.

(3) In our sample, the early-type disc galaxies (S0/a) have both flat and 'puffed' discs. The early spirals and intermediate-type galaxies have a large scatter of the disc flatness, which can be caused by the presence of a bar: barred galaxies have thicker stellar discs, on average. On the other hand, the late-type spirals are mostly thin galaxies, whereas irregular galaxies have puffed stellar discs.

Key words: galaxies: statistics – galaxies: structure.

1 INTRODUCTION

Morphological and photometric characteristics of galaxies vary along the Hubble sequence (see the review by Roberts & Haynes 1994). Contribution of the bulge to the total luminosity of a galaxy decreases, galaxies tend to be bluer, spiral pattern gets less tightly wound, the fraction of gas increases while going from early- to late-type galaxies.

Guthrie (1992) analysed the distribution of isophotal axial ratios in a large sample of Uppsala General Catalogue (UGC, Nilson 1973) galaxies to study true axial ratios b/a and found the dependence of the true axial ratio on the morphological type and that the late-type galaxies have smaller b/a. Karachentsev et al. (1997) measured the apparent axial ratios b/a of galaxies from the Flat Galaxies Catalogue (Karachentsev, Karachentseva & Parnovsky 1993) and found that the flat galaxies exhibit the dependence of the flattening on the morphological type: galaxies of the late types are flatter.

Although the apparent axial ratio is an indicator of the disc thickness, these two characteristics are not the same. de Grijs (1998) performed the 1D photometric profile analysis for 45 edge-on galaxies and derived global galaxy parameters in three photometric bands (optical and near-infrared). He found a correlation between the ratio of the radial to vertical scale parameter and galaxy type: galaxies become systematically thinner when going from the type S0 to Sc. According to de Grijs (1998), the ratio of the radial scalelength h to the vertical scaleheight z_0 in his sample of edge-on galaxies varies from 1.5–2 in the early-type spirals to 3–8 in the Sc–Sd galaxies. Note, however, that the scatter in z_0/h is large for any certain morphological type.

Kregel, van der Kruit & de Grijs (2002) re-analysed the *I*-band photometry of 34 edge-on spiral galaxies from the sample by de Grijs (1998). They applied a 2D algorithm to derive the scale parameters of the stellar disc and, thereby, the disc flattening. They also

★ E-mail: mosenkovAV@gmail.com (AVM); nsot@astro.spbu.ru (NYS)

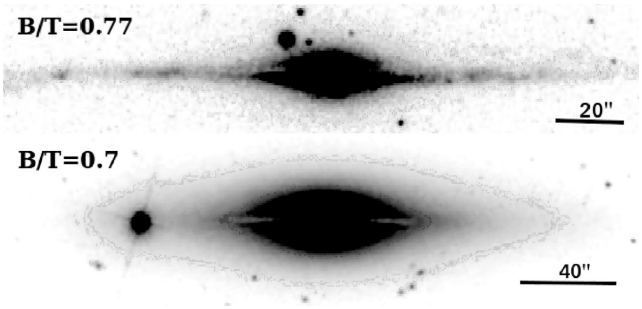

Figure 1. Examples of galaxies from the EGIS catalogue (*i* band): IC 3608, Sb (Sab as given in the Catalogue of Detailed Visual Morphological Classifications for 14 034 Galaxies in SDSS; Nair & Abraham 2010), $z_0/h = 0.10$, bulge-to-total luminosity ratio B/T = 0.77 (top), and NGC 1032, S0/a (Sa in the Uppsala General Catalogue of Galaxies; Nilson 1973), $z_0/h = 0.30$, B/T = 0.70 (bottom). The morphological types are taken from the HyperLeda data base. The parameters are estimated via the 2D bulge/disc decomposition using DECA package (Mosenkov 2014) with masking the central dust lanes (see Section 3.1 and also Fig. 4).

used the revised Hubble types of the galaxies from the HyperLeda data base, which were significantly shifted around as compared with those used by de Grijs (1998), sometimes by more than one subtype. However, Kregel et al. (2002) did not use the revised data to discuss the dependence of the ratio z_0/h on the morphological type found earlier by de Grijs (1998) on the base of the same sample. It was done by Hernandez & Cervantes-Sodi (2006), who analysed the data by Kregel et al. (2002) and confirmed a diminishing trend of the ratio z_0/h while going from the early to late types: the late-type galaxies at the Sc end have thinner discs than the earlier types, on average. Careful examination of fig. 7 in Hernandez & Cervantes-Sodi (2006) shows that the trend is supported by only one point (a galaxy of Sa type). Therefore, we can conclude that the reported correlation is rather poor.

Ma et al. (1997, 1999) and Ma, Peng & Gu (1998) explored some statistical correlations for spiral galaxies of intermediate inclinations. They measured the disc thickness by the method proposed by Peng (1988). The method for determining the thickness of a spiral galaxy is based on the solution of Poisson's equation for a logarithmic disturbance of density. Ma et al. (1997, 1998, 1999) showed that the ratio of the vertical to radial scales in the stellar disc tends to decrease along the Hubble sequence. It is important to note that all mentioned results are based on indirect methods for determining the disc flatness, on a simple 1D photometric profile analysis or on limited data sets.

Bizyaev et al. (2014, hereafter BKM14) created the Edge-on Galaxies in SDSS (EGIS) catalogue, a catalogue of edge-on galaxies in the Sloan Digital Sky Survey (SDSS). In their 3D photometric analysis of 5747 edge-on galaxies selected from SDSS Data Release 8, they did not find significant correlation between the disc flatness and the morphological type. Moreover, a visual inspection of galaxy images shows that early-type galaxies may have very flattened, as well as 'puffed' discs (see Fig. 1). Bizyaev & Kajsin (2004) also noticed the existence of very thin stellar discs in galaxies with large bulges.

To sort out this question, we analyse the dependence of the stellar disc flatness on the galaxy morphological type using robust 2D decomposition results obtained for a representative subsample of the EGIS catalogue. We also use the results of studying edge-on galaxies from the Two Micron All Sky Survey (2MASS) archive (Mosenkov, Sotnikova & Reshetnikov 2010, hereafter MSR10) and from the Spitzer Survey of Stellar Structure in Galaxies (S^{4}G; Sheth et al. 2010).

This paper is organized as follows. In Section 2, we describe our methodology of the 2D bulge/disc decomposition. We show that the approach used for decomposing edge-on galaxies brings up statistically reliable results. In Section 3, we introduce the samples of galaxies which are considered in this work. In Section 4, we present the results of our analysis, namely the correlations between the disc flatness and other quantities such as the morphological type, bulge-to-total luminosity ratio, galaxy colour, and galaxy luminosity. In Section 5, we discuss why the results of this article contradict the results of previous investigations. We also make some comments on the physical sense of the lack of the correlation between the disc flattening and the galaxy morphological type. In Section 6, we summarize our main conclusions. The cosmological framework adopted throughout this paper is $H_0 = 70\,\mathrm{km\,s^{-1}\,Mpc^{-1}}$, $\Omega_\mathrm{m} = 0.3$, and $\Omega_\Lambda = 0.7$.

2 THE DECOMPOSITION TECHNIQUE

We first describe the main decomposition technique employed in this study to analyse the structure of edge-on galaxies. There are three methods for decomposing such objects widely used in the structural analysis: the one-dimensional (1D; e.g. de Grijs 1998; Bizyaev & Mitronova 2002; BKM14), two-dimensional (2D; see Simard et al. 2002; de Souza, Gadotti & dos Anjos 2004; Peng et al. 2010), and three-dimensional method (3D; see, for example, Xilouris et al. 1999; Bianchi 2007; Baes et al. 2010; BKM14).

The 1D methods applied to edge-on galaxies considers photometric profiles along the major and minor axes independently. In contrast to that, in 2D fitting the whole information from the 2D image is used simultaneously to build a robust model for each galactic component. There are several examples in the literature showing that the 2D method is much more reliable than the 1D method (e.g. de Jong 1996) in retrieving the accurate structural parameters. In the 3D method, a dust extinction model is usually adopted, which makes this method more precise but rather time consuming. Since proper treatment of radiative transfer models takes significant computational resources (Bianchi 2007; Baes et al. 2010; De Looze et al. 2012), various simplifications can be applied (BKM14). In this section, we briefly describe the adopted 2D technique in the comparison with the 1D and 3D methods in Section 5.1.

2.1 The 2D decomposition

The 2D photometric decomposition of galactic images is realized in a number of packages such as GIM2D (Simard et al. 2002), GALFIT (Peng et al. 2002, 2010), BUDDA (de Souza et al. 2004), and IMFIT (Erwin 2015). In this work, we use three of them: BUDDA, IMFIT, and the most famous code GALFIT. Although the minimization algorithms are different in these packages, we assume they bring similar results of the decomposition since they have been tested and compared by different authors (e.g. Häussler, McIntosh & Barden 2007; Häussler et al. 2013; Busch et al. 2014; Kim et al. 2014). Also, each of these codes has its advantages which will be noticed further.

To perform the bulge/disc decomposition, new Python wrapper DECA[1] was made, as described in detail by Mosenkov (2014). The DECA software package was designed to perform photometric analysis of the structure of regular galaxies, with the simple automatic

[1] http://lacerta.astro.spbu.ru/?q=node/96

decomposition on to bulge and disc using GALFIT as the galactic model generator. It also takes advantages of several widely used packages such as IRAF, SExtractor and several PYTHON libraries as, for example, PYFITS. DECA requires minimal human intervention as no any initial values of the bulge or disc parameters should be given. The algorithm is built in the way that it uses the input image of the studied galaxy (or, it may be a field with many different objects), the point spread function (PSF) image, and the input text file with the main information about the object (equatorial coordinates RA and DEC, redshift, and colour) and the frame calibration (photometric zero-point, pixel scale, gain, etc.).

A simple model of an edge-on disc galaxy represents a superposition of two photometric components: the bulge and the edge-on disc. The distribution of the surface brightness in the radial r and vertical z directions for the transparent 'exponential' disc observed at the edge-on orientation is described by the following expression:

$$I(r,z) = I(0,0)\frac{r}{h}K_1\left(\frac{r}{h}\right)\mathrm{sech}^2(z/z_0), \quad (1)$$

where $I(0, 0)$ is the disc central intensity, h is the radial scale-length, z_0 is the 'isothermal' scaleheight of the disc (Spitzer 1942; van der Kruit & Searle 1981a,b, 1982a,b), and K_1 is the modified Bessel function of the first order. To find the edge-on disc central surface brightness, we should calculate $I_0^{\mathrm{edge-on}} = \int_{-\infty}^{\infty} I(r,0)\mathrm{d}r$ (designated as $\mu_{0,\,\mathrm{d}}$ if expressed in mag arcsec^{-2}).

The bulge profile is given by the Sérsic law (Sérsic 1968):

$$I(r) = I_{0,\,\mathrm{b}}\,\mathrm{e}^{-\nu_n(r/r_{\mathrm{e,b}})^{1/n}}, \quad (2)$$

where $r_{\mathrm{e,\,b}}$ is the effective radius, or the half-light radius, $I_{0,\,\mathrm{b}}$ is the central surface brightness (it can be reduced to the effective surface brightness $\mu_{\mathrm{e,\,b}}$ expressed in mag arcsec^{-2}), n is the Sérsic index defining the shape of the profile, and the parameter ν_n depending on n ensures that $r_{\mathrm{e,\,b}}$ is the half-light radius.

In order to estimate the bulge-to-total luminosity ratio B/T, we can find the total luminosity of the bulge and the disc via integrating the equations (1) and (2) over the whole galaxy image.

DECA also allows us to take into account the stellar disc truncation when needed. The axis ratio of the bulge q_{b} and its ellipticity parameter that controls the shape of the bulge ('boxy' or 'discy') can be set as free parameters.

2.2 Robustness of the DECA decomposition

As the main aim of this work is studying edge-on galaxies selected from SDSS, we tested DECA on the sample of artificially created galaxy images that imitate SDSS images in the i band with the typical for the EGIS galaxies signal-to-noise ratio. We generated a galaxy image as the sum of photometric disc and bulge components by using expressions (1) and (2), respectively. We built a sample of 1000 artificial images with the uniform distributions of the parameters similar to those from Kregel et al. (2002). The boundary values for each parameter are taken from the physical background summarized in several works (e.g. Gadotti 2009; MSR10). The disc parameters cover the following ranges:

$16 \leq \mu_{0,\mathrm{d}} \leq 21\,\mathrm{mag\,arcsec}^{-2}$,

$0.5 \leq h \leq 10\,\mathrm{kpc}$,

$0.1 \leq z_0 \leq 1.5\,\mathrm{kpc}$.

For bulge, the ranges are as follows:

$18 \leq \mu_{\mathrm{e,b}} \leq 22\,\mathrm{mag\,arcsec}^{-2}$,

$0.1 \leq r_{\mathrm{e,b}} \leq 2\,\mathrm{kpc}$,

$0.5 \leq n \leq 5$,

$0.5 \leq q_{\mathrm{b}} \leq 1.0$.

The image scale varied randomly between 0.4 and 2 kpc arcsec^{-1}. The simulated images of galaxies were created using the PYTHON wrapper SIGAL[2] which operates the GALFIT code to produce model images. All created images were convolved with the Moffat PSF with FWHM = 1.2 arcsec. The pixel size is 0.396 arcsec pixel^{-1}, the exposure time was set to 53.9 s and the gain is 4 e$^-$ ADU^{-1}. We added Gaussian readout noise and poison noise to each pixel of the image. All galaxy discs were truncated up to the distance of 4 h.

The decomposition of the artificial galaxy images was then performed with the DECA package. The robustness of the decomposition is shown in Fig. 2 for the parameters B/T and z_0/h which are of great interest for us in this paper. We can see that for galaxies with a semimajor axis (being estimated as the truncation radius of the galaxy) larger than 20 arcsec $\langle(\Delta\mathrm{B/T})/(\mathrm{B/T})\rangle = 0.01 \pm 0.23$ and $\langle(\Delta z_0/h)/(z_0/h)\rangle = 0.017 \pm 0.06$ while for galaxies with the lesser semimajor axis $\langle(\Delta\mathrm{B/T})/(\mathrm{B/T})\rangle = 0.077 \pm 0.55$ and $\langle(\Delta z_0/h)/(z_0/h)\rangle = 0.05 \pm 0.18$. Therefore, we conclude that the minimum diameter of a galaxy with B/T > 0 to be well decomposed is $D^i_{\mathrm{min}} \approx 40$ arcsec (hereafter, we put the upper index to designate the passband). For galaxies with the diameter larger than D_{min}, we may expect that the average errors for the fitted parameters z_0/h and B/T should be less than 10 and 25 per cent of their true values, respectively. Thus, the results of our test confirm the robustness of fitting performing by DECA and its possibility for decomposing large sets of galaxies imaged by SDSS.

3 THE SAMPLES AND THE DECOMPOSITION

Our further analysis is based on the study of several samples of galaxies viewed almost perfectly edge-on ($i \geq 86^\circ$) that were observed in different passbands. Although we focus our study on the sample of galaxies selected from SDSS, we also use the results of several investigations in near- and mid-infrared bands.

The SDSS (Aihara et al. 2011) is an ambitious project to investigate the Universe in five optical passbands. Because the dust extinction along the major axis of the disc is substantially high in these bands, the vast majority of edge-on galaxy images demonstrate very well seen dust lanes. Hence, the proper model fitting of such galaxies should be carried out with taking into account the radiative transfer approach (e.g. Xilouris et al. 1999) which can be done for galaxies with sufficient spatial resolution (for nearby edge-on galaxies if we use SDSS) and takes significant computational time. Nevertheless, as we will show later, some galaxies (of both early and late types) do not demonstrate sharp dust lanes in optics, and thus they can be decomposed using standard fitting packages described in Section 2. Galaxies with dust traces (having no sharp dust lanes) can be also decomposed using masking of these regions of high dust extinction.

Since in the near-infrared (*JHK*) and mid-infrared *Spitzer* bands *W*1 (3.6 μm) and *W*2 (4.5 μm) the flux is largely dominated by the stellar radiation rather than gas and dust emission (Whaley et al. 2009), and the dust extinction here is much less than in optics, it is crucial to investigate the structure of the stellar discs and bulges in

[2] https://github.com/latrop/SIGAL

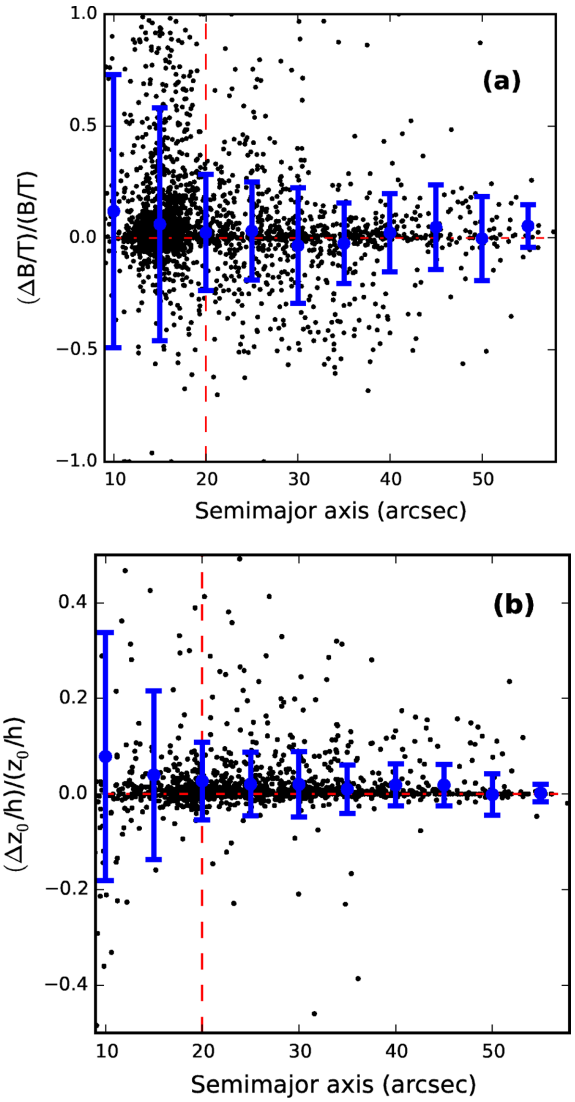

Figure 2. Results of simulations as a function of the semimajor axis size of the artificially created edge-on galaxy images for the SDSS, *i* band. (a) The distribution of $(B/T - B/T_{fit})/(B/T)$, where B/T is a known and B/T_{fit} is a fitted bulge-to-total luminosity ratio. (b) The distribution of $(z_0/h - z_0/h_{fit})/(z_0/h)$, where z_0/h is a known and z_0/h_{fit} is a fitted disc flattening. The limiting radius is estimated to be about 20 arcsec (designated as the vertical red dashed line), or $D^i_{min} = 40$ arcsec. The ordinates for each plot were averaged inside the bin of 5 arcsec (blue circles with the bars representing the standard deviation of the parameters inside each bin). The horizontal red dashed line corresponds to the zero value of the ordinate.

these bands. Because of these aspects, the use of 2MASS (Skrutskie et al. 2006) and S^{4}G (Sheth et al. 2010) is suitable for our aims.

In order to select edge-on galaxies from existing catalogues and data bases, we will use a selection criterion based on the galaxy apparent diameter at a given isophotal level. This allows us to select galaxies in the same manner. As was noticed in Section 2.2, the value of the limiting apparent galaxy diameter for each sample should be chosen so as to exclude galaxies with poor bulge/disc decomposition. In Section 2.2, we found that $D^i_{min} = 40$ arcsec if we consider galaxy images in SDSS. Supposing that the main factor that affects the quality of bulge/disc decomposition is the image resolution and PSF (as reflected by the pixel size in arcsec), we can estimate the minimum diameter of 2MASS and S^{4}G galaxies to be well decomposed by scaling our estimates performed for SDSS case. The pixel size in 2MASS is 2.5 times larger than in SDSS, hence the limiting apparent diameter should be $D^{Ks}_{min} = 100$ arcsec. In the case of S^{4}G where the pixel size is 0.75 pixel arcsec^{-1}, $D^{3.6}_{min} = 75$ arcsec.

In our study, we consider only two main galactic components: the bulge and the disc, for simplicity. Possible influence of the multicomponent structure of edge-on galaxies on the main results of this work will be discussed in Section 5.3.

The galaxy morphological type (*Type*) and the colour $B - I$ for each galaxy were taken from the HyperLeda data base (Paturel et al. 2003). The *B* and *I* bands are close to the *g* and *i* bands, respectively, therefore we opt to use the colour $B - I$ for 2MASS and S^{4}G galaxies along with the colour $g - i$ for SDSS galaxies.

Each galaxy from the samples was visually inspected whether its shape resembles the shape of edge-on galaxies. Images in different passbands available in the NASA/IPAC Extragalactic Database (NED) were analysed to check the presence of a dust lane along the edge-on disc. For all galaxies of the samples, we retrieved inclination angle *i* from the HyperLeda and found the mean value of all galaxies studied $\langle i \rangle = 88.^\circ0 \pm 3.^\circ5$. In Appendix A, we describe how we estimated the inclination angle in an independent way.

Fig. 3 demonstrates the distribution of the total galaxy luminosities in our samples. We ensure that the galaxies used for the analysis are non-dwarf and luminous. Detailed description of the samples is given below.

3.1 The SDSS sample

In order to select comparatively large edge-on galaxies from SDSS, we used the EGIS catalogue which is described in detail by BKM14. This is the largest catalogue of verified edge-on galaxies at the moment which comprises 5747 genuine edge-on galaxies pre-selected automatically from the SDSS Data Release 8 and then visually inspected. This catalogue is complete for all galaxies with the major axis D^i larger than 28 arcsec (see BKM14) and comprises disc galaxies of all morphological types (Sa–Sd-Irr), which is important for studying galaxies of different bulge contribution.

In Section 2.2, we concluded that the minimum diameter of galaxies for keeping our decomposition robust is 40 arcsec. Therefore, from the EGIS catalogue we selected objects with $D^i > 40$ arcsec and excluded galaxies with irregular structure of discs and with various contaminants as bright overlapping stars or galaxies. This resulted in the initial sample of 2027 objects. After a thorough visual inspection and preliminary decomposition of each galaxy image in the *i* band, we selected 145 galaxies and then estimated their inclination angle using two methods described in Appendix A. We applied the first method to the galaxies without dust traces and the second method to the galaxies with visible dust manifestations. After that, we removed four galaxies with $i < 86^\circ$. Therefore, the final sample includes 82 galaxies without any presence of dust lanes and 59 galaxies with slightly visible dust lanes. The mean inclination angle for the galaxies in our sample is $\langle i \rangle = 88.^\circ2$. An evidence that a galaxy has no strong dust attenuation came from the inspection of residual images ('galaxy'−'model') and browsing of the vertical and radial photometric profiles. Since no dust traces were found in their profiles, we may hope that structural decomposition of these galaxies based on the model of transparent disc is more robust than for the rest of the sample. We will call this subsample of 82 'dust-free' galaxies the 'reference subsample'. The selected sample consists of 27 early-type ($T \leq 0$) and 114 late-type galaxies ($T > 0$).

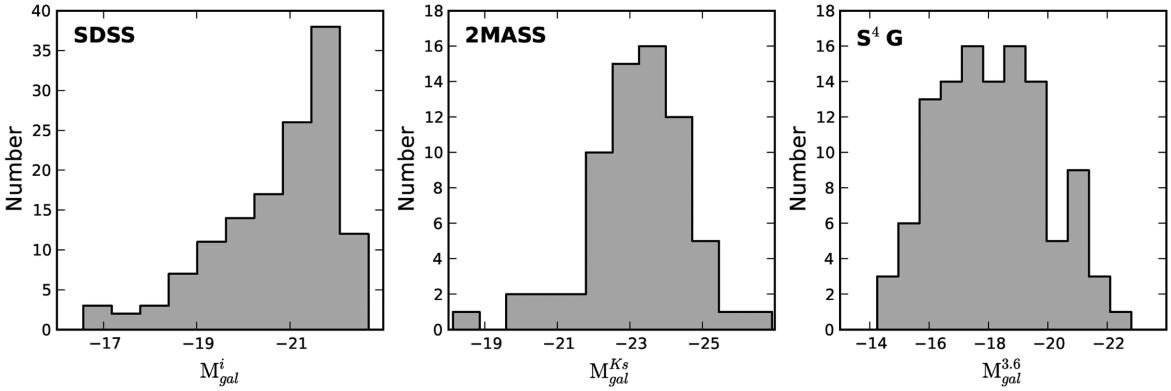

Figure 3. The distributions of the total luminosity for the galaxies from SDSS (i band), 2MASS (K_s band), and S^{4}G (3.6 μm) samples.

The redshifts retrieved from the SDSS Data Release 9 prove that the galaxies of the sample are nearby ($z < 0.05$, $\langle z \rangle = 0.02$).

The 2D decomposition of the galaxy images from the sample of all 141 objects was performed using the DECA code. The i-band images were downloaded from the SDSS Data Release 9 (Ahn et al. 2012). PSF (prefix 'psField') images were retrieved from the SDSS Data Archive Server. If a prominent dust lane was seen in the galaxy image (as for NGC 1032 in Fig. 4), it was masked during the decomposition.

We checked our sample for completeness and found that the subsample of 98 galaxies with $D^i > 48$ arcsec is complete while the whole sample is incomplete according to the $V/V_{\rm max}$ test (Thuan & Seitzer 1979). In Fig. 5, left-hand panel, we can see that the distribution of the apparent axis ratio in the sample (grey colour) and in the whole EGIS catalogue (red solid line) are very similar. We performed the Kolmogorov–Smirnov test to verify the null hypothesis that these two samples are drawn from the same population. We found that we cannot reject the null hypothesis at a 5 per cent or lower α since the p-value is high and equals to 0.88. If the distributions of galaxy luminosity (Fig. 5, middle plot) and colour are considered, (Fig. 5, right-hand plot), we can also see that these distributions look similar for both samples. However, according to the Kolmogorov–Smirnov test there is no sufficient evidence to reject the null hypothesis (for the $M^i_{\rm gal}$ distribution: $\alpha = 0.105$, p-value $= 0.12$; for the $g - i$ distribution: $\alpha = 0.09$, p-value $= 0.14$). Since the apparent axis ratio, galaxy total luminosity, and colour are the main photometrical characteristics of the observed objects, the distributions of these parameters for the sample of 141 galaxies and the EGIS catalogue are similar, we may conclude that our sample well represents the whole EGIS catalogue.

3.2 The 2MASS sample

In order to create another sample of genuine edge-on galaxies, we used a sample described in detail in MSR10. The 2MASS sample from MSR10 contains galaxies with a wide range of bulge contribution: from galaxies with prominent bulges to bulgeless galaxies. To select the galaxies, we used the 2MASS-selected Flat Galaxy Catalogue (2MFGC, Mitronova et al. 2003) and the Revised Flat Galaxy Catalogue by Karachentsev et al. (1999). Galaxies were selected from the 2MFGC according to the following criteria: the axial ratio $sba > 0.2$, the K_s-band Kron radius $R^{K_s} \geq 30$ arcsec and the concentration index (which is connected to the bulge-to-disc luminosity ratio) IC > 2.0. The interacting, peculiar, and non-edge-on galaxies identified visually and according to the information found in HyperLeda, were removed from our consideration. The final sample consists of 175 galaxies in the K_s band, with images taken from the 2MASS archive. All the galaxies were decomposed into a bulge and a disc using the BUDDA code (de Souza et al. 2004, see several examples of decomposition in MSR10).

We found that about one-third out of the sample of 175 galaxies have inclinations less than 86° as estimated using the first method described in Appendix A. We removed these galaxies, as well as the galaxies with the diameter smaller than $D^{K_s}_{\rm min} = 100$ arcsec. The resulting sample comprises 66 large genuine edge-on galaxies.

According to the $V/V_{\rm max}$ test, our final sample is incomplete and thus may suffer selection effects. In the left-hand panel in Fig. 6, we can see that the distribution of the final sample (grey colour) and the distribution of the whole 2MASS sample over the apparent axis ratio differ since we excluded non edge-on galaxies from subsequent analysis – these galaxies form a peak at $b/a = 0.32$ (the red line distribution). The other distributions (middle and right panels) do not show significant differences between the initial sample of 175 galaxies and the final one. The selected sample comprises 10 early-type and 56 late-type galaxies. All the galaxies are nearby, with $z < 0.035$ (average redshift $\langle z \rangle = 0.007$); the mean inclination angle is $\langle i \rangle = 88.^\circ 0$.

3.3 The S^{4}G sample

The S^{4}G catalogue consists of 2352 nearby (with distance less than 40Mpc) galaxies at 3.6 and 4.5 μm, and it is a valuable source of edge-on galaxies. Using the S^{4}G Galfit Models Home Page[3], we retrieved the best decomposition models with the edge-on disc included in 362 galaxies (at 3.6 μm). However, the visual inspection of the *Spitzer*, DSS, and SDSS images of these galaxies showed that some galaxies are not quite edge-on since they have round elliptical isophotes, or visible spiral arms, or rings), therefore we did not classify these galaxies as edge-on (for example, NGC 5984 and NGC 678). Otherwise, we would risk to retrieve false thicker stellar discs, which can significantly mislead us in studying the dependence between the disc flattening and the galaxy morphological type.

From the pre-selected sample of edge-on galaxies in the S^{4}G model catalogue, we selected galaxies consisted either of the disc alone (late types), or of the disc and the bulge (early and intermediate types[4]). Galaxies with detected double-exponential discs

[3] The catalogue of galactic structural parameters can be found at http://www.oulu.fi/astronomy/S4G_PIPELINE4/s4g_p4_table8.dat.
[4] 31 galaxies were fitted with the 'bulge+disc' model

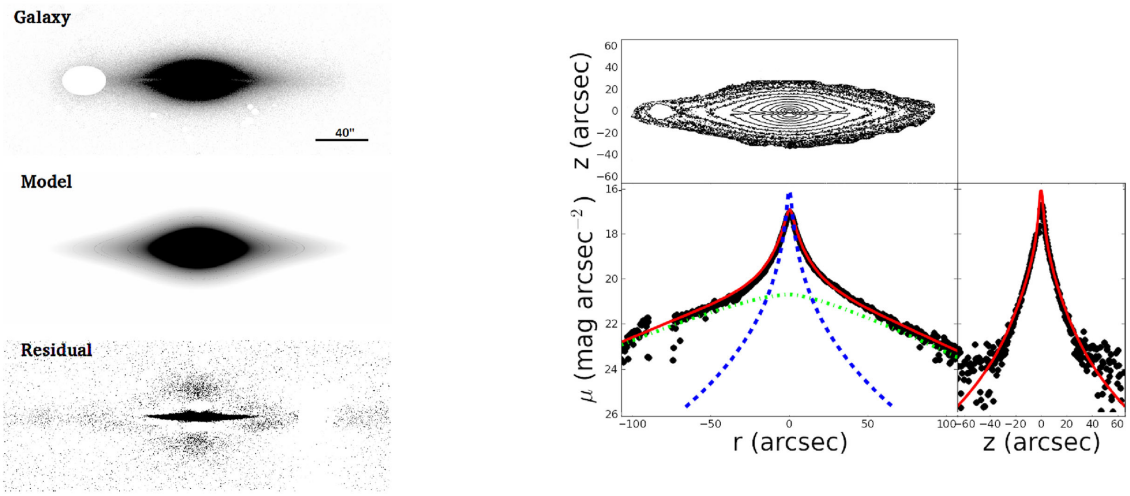

Figure 4. The decomposition of the S0/a edge-on galaxy NGC 1032 using the DECA code (SDSS, *i* band). Left-hand panel shows the galaxy image (top), the model (middle) and the residual image ('galaxy'−'model', bottom). Right-hand panel represents the isophote map of the galaxy down to the 22.5 mag arcsec^{-2} surface brightness (top), the photometric cut along the major axis (bottom left), and the photometric cut along the minor axis (bottom right). The black dots refer to the galaxy, the red solid line represents the model, the blue dashed line represents the bulge, and the disc is shown by the green dots. The dust lane was masked during the decomposition. Main derived parameters of the decomposition are B/T = 0.70, $z_0/h = 0.30$.

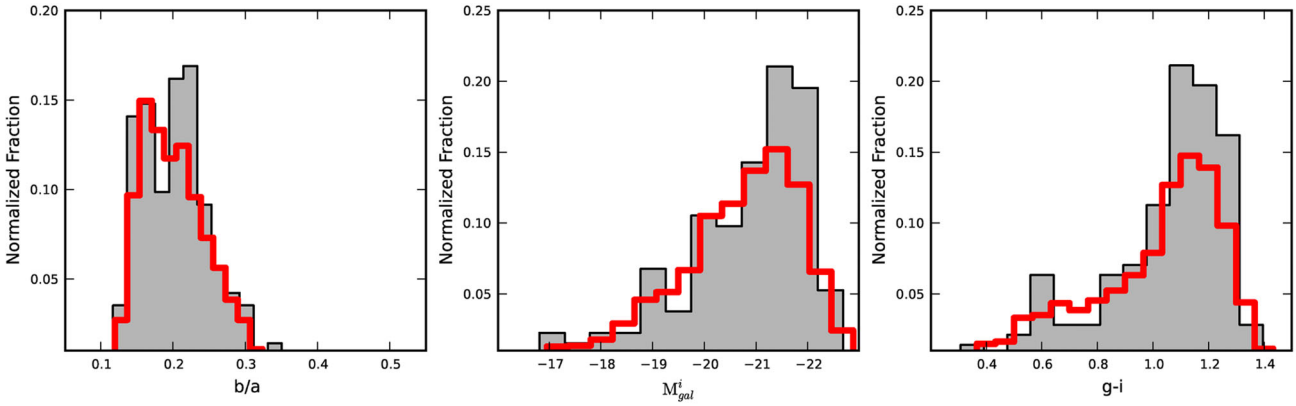

Figure 5. The distributions of the apparent axis ratio, total luminosity, and colour for the selected SDSS sample (grey) and the EGIS catalogue (red solid line).

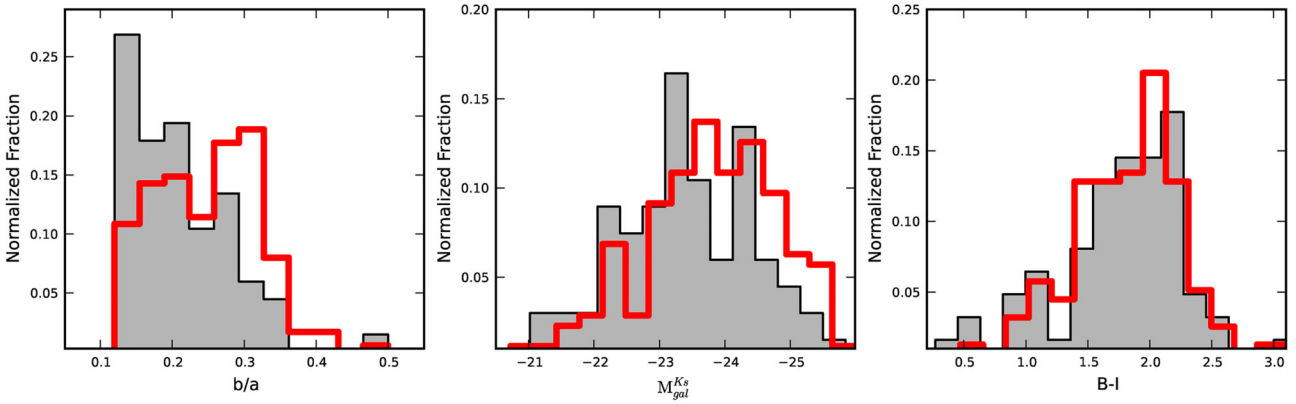

Figure 6. The distributions of the apparent axis ratio, total luminosity, and colour for the selected 2MASS sample (grey) and the sample from MSR10 (red solid line).

are not considered in this work. Then, we estimated inclinations of the selected galaxies using the first method from Appendix A and removed objects with $i < 86^\circ$. Also, we removed non-bulgeless galaxies with smaller than minimum diameter at the outer isophote of $W1 = 25.5$ mag arcsec^{-2} $D^{3.6}_{25.5} < D^{3.6}_{\rm min}$, where $D^{3.6}_{\rm min}$ was estimated to be 75 arcsec.

The total number of edge-on galaxies of all types selected from the S^{4}G model catalogue is 99, with the mean inclination angle

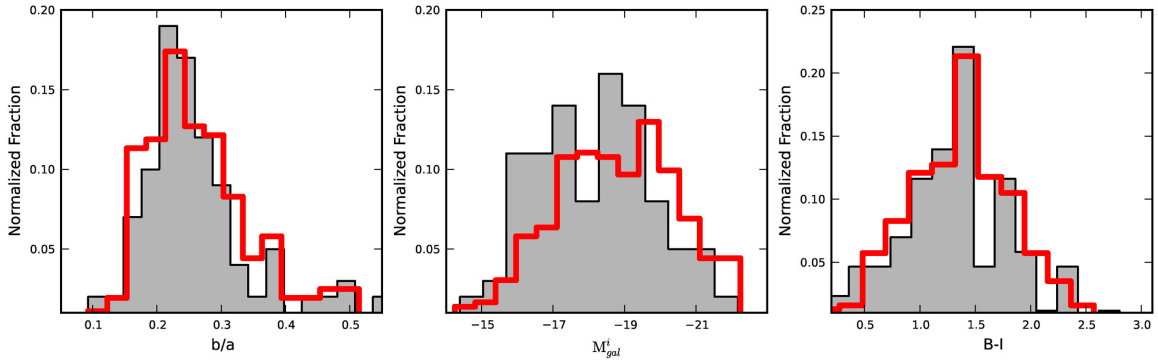

Figure 7. The distributions of the apparent axis ratio, total luminosity, and colour for the selected S^{4}G sample (grey) and the whole sample of 362 edge-on galaxies in the S^{4}G catalogue (red solid line).

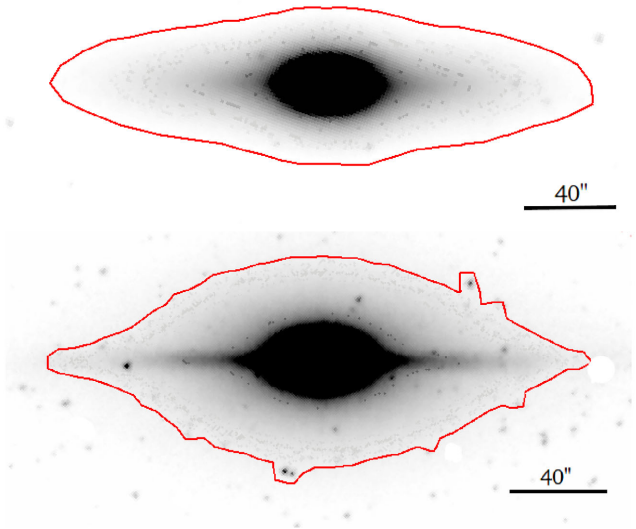

Figure 8. Examples of early-type galaxies from the S^{4}G data base ($W1$ band): NGC 1596 (S0, $z_0/h = 0.34$, B/T = 0.64, top) and NGC 7814 (Sab, $z_0/h = 0.15$, B/T = 0.90, bottom). The disc thicknesses and bulge-to-total luminosity ratios are taken from S^{4}G Galfit Models Home Page. The red contours refer to the outer isophote of $W1$=25.5 mag arcsec^{-2}.

$\langle i \rangle = 87.^\circ9$. The sample mostly consists of the late-type galaxies (8 early-type and 91 late-type galaxies). We did not reject galaxies of the latest morphological types (23 irregular galaxies, with poorly defined structure) though we assume that their edge-on orientation determination is rather precarious. We make some comments on this issue in the further sections.

In Fig. 7, we show the distributions for the selected sample (grey colour) and the whole sample of 362 galaxies decomposed with edge-on discs in the S^{4}G catalogue (the red line distribution). It is well seen that all present distributions are very similar. However, the distribution of $M^i_{\rm gal}$ shows that our S^{4}G sample comprises larger number of low-luminosity galaxies and less number of high-luminosity galaxies in the comparison with the whole sample of edge-on galaxies in the S^{4}G catalogue.

Although our S^{4}G sample is significantly incomplete according to the $V/V_{\rm max}$ test and different morphological types are not statistically representative in the sample, this is the only sample of genuine edge-on galaxies observed in the mid-infrared bands (see examples of the edge-on galaxies from the created S^{4}G sample in Fig. 8), thus we consider this sample carefully in this work.

4 RESULTS

4.1 The disc thickness versus the morphological type

First, let us consider the dependence of the disc relative thickness z_0/h on the galaxy type. In fig. 14 from BKM14, one can see the dependence between the stellar disc thickness and the type derived from the 1D analysis. This dependence is similar to that found in de Grijs (1998) also based on the analysis of 1D photometric profiles. At the same time, the 3D analysis for the same sample (see fig. 15 in BKM14) does not allow us to conclude that this dependence truly exists. It only shows that the late-type edge-on galaxies (determined as galaxies without bulge) are thinner than others, on average. Thus, we can conclude that a more advanced 3D method of decomposition erases the thickness-type dependence.

It is worth noticing that morphological types in BKM14 were estimated automatically for each galaxy using main photometrical parameters from SDSS. We compared these types with those extracted from the HyperLeda data base and found the mean scatter between these two systems of morphological classification being two T-units.

Fig. 9 shows the distribution of the galaxies from our SDSS, 2MASS, and S^{4}G samples in the same z_0/h–*Type* space. The SDSS sample is shown in Fig. 9, the top panel. We also marked here the galaxies with dust traces (open circles) and with visible X-shaped structure (red crossed symbols) which are candidates to hosting bars as discussed by Bureau et al. (2006). The whole sample demonstrates a trend (the Pearson's correlation coefficient $\rho = -0.56$, the two-sided p-value p = 1.44e-12). The difference in the thickness between the thickest and the thinnest discs is of the factor of 1.5.

For the 2MASS sample of large galaxies, we do not see strong variations of the relative thickness with the morphological type ($\rho = -0.41$, $p = 0.001$; see Fig. 9, middle plot). Since the S^{4}G sample consists mainly of late-type edge-on galaxies (many of them occur to be irregular), we have even an upward trend for the galaxies with $T > 6$ (blue dashed regression line with $\rho = 0.48$ and $p = 0.016$ on Fig. 9, bottom panel). For the galaxies with $T \leq 6$, the correlation between z_0/h and *Type* is not seen ($\rho = -0.15$, $p = 0.443$). Notwithstanding small number of early-type galaxies and excluding irregular galaxies with $T \geq 8$, the overall picture does not reveal any correlation between the morphological type and the stellar disc flattening.

The poor dependence between the disc flattening and the galactic morphological type is confirmed indirectly by Chudakova & Silchenko (2014). The latter paper presents a new photometric method for deriving the relative thickness of the stellar disc from

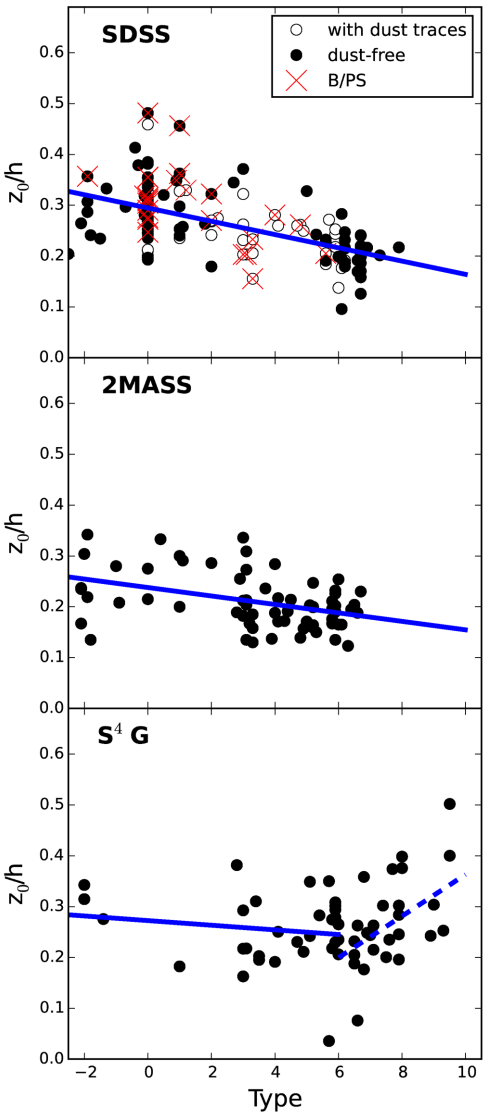

Figure 9. The distribution of the disc flatness as a function of the morphological type for the SDSS (top panel, *i* band), 2MASS (middle panel, K_s band), and S^{4}G (bottom panel, 3.6 μm) sample. The open circles in the top panel refer to the subsample of galaxies with slightly visible dust lanes (59 galaxies). The filled circles refer to the reference subsample of galaxies without dust lanes (82 galaxies). The red crosses mark the galaxies with sharp X-pattern structures in the central region. The blue lines represent the regression lines for each sample (see the text).

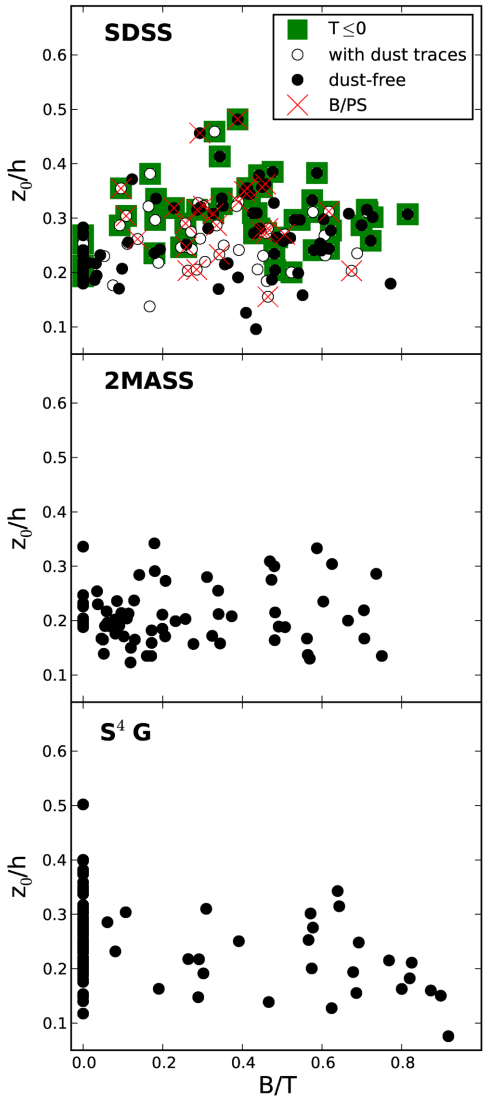

Figure 10. The distribution of the stellar disc flatness as a function of the bulge-to-total luminosity ratio for the SDSS (*i* band), 2MASS (K_s band), and S^{4}G (3.6 μm) samples. Symbols as in Fig. 9, and the green squares represent early-type galaxies with *Type* ≤ 0.

2D surface brightness photometry. The method was applied to a sample of 45 early-type (S0-Sb) galaxies. They found that the discs of lenticular and early-type spiral galaxies have similar thickness, on average.

4.2 The disc thickness versus the bulge-to-total luminosity ratio

Determination of the morphological type for edge-on galaxies is difficult. van den Bergh (1998) in his review on the galactic morphology and classification stressed that edge-on galaxies are often difficult or impossible to classify. Naim et al. (1995) concluded that the agreement between independent observers to do morphological classification is good, on average, but the scatter is large (about 1.8 subtypes). However, in the case of edge-on galaxies the agreement between independent classifiers is worse (see fig. 6, right-hand panel in that work). In Section 5.2, we will demonstrate how the inclination of a galaxy can affect its morphological classification.

For edge-on galaxies, it is more reliable to use the bulge-to-total luminosity ratio B/T as the indicator of the galaxy morphological type because this value can be estimated directly from the photometric analysis and modelling.

In Fig. 10, we plotted the dependence of the disc relative thickness z_0/h on the bulge-to-total luminosity ratio B/T. One can see that for galaxies from SDSS (the top panel) with $0.2 \lesssim \mathrm{B/T} \lesssim 0.6$ there is a large scatter of z_0/h values around $z_0/h \approx 0.3$. The galaxies with visible X-shaped structures (red crosses) lie within the same limits $0.2 \lesssim \mathrm{B/T} \lesssim 0.6$ with the relative thickness $z_0/h \approx 0.30 \pm 0.05$ in comparison with the average flatness for the whole sample $\langle z_0/h \rangle = 0.25 \pm 0.07$. Thus, we may conclude that the galaxies with X-shaped structures have thicker stellar discs, on average.

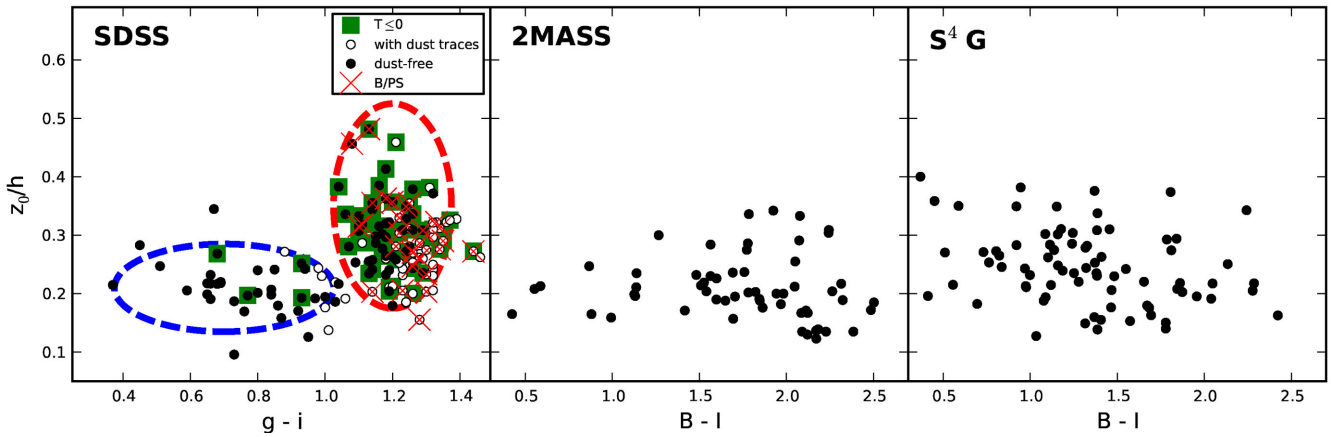

Figure 11. The distribution of the disc flattening as a function of the colour $g - i$ for the SDSS (i band), 2MASS (K_s band), and S^{4}G (3.6 μm) sample. The red and blue ovals outline the two possible families of galaxies selected from their loci on the $g - i$–z_0/h plane. The symbol designation is kept the same as in Fig. 10.

We verified whether our fitting procedure could affect the possibly existed correlation between z_0/h and B/T taking into account the fact that these retrieved parameters may have 10 and 25 per cent uncertainties respectively (see Section 2.2). We created a simulated sample with the same distribution of z_0/h as for the SDSS sample, where there exists correlation between the disc flatness and the bulge-to-total luminosity ratio with the regression coefficient $\rho = 0.55$. We then applied the biasing to each point in the B/T–z_0/h space using the normal distributions with the standard deviations $0.25 \cdot B/T$ and $0.1 \cdot z_0/h$ for the values of B/T and z_0/h, respectively. We repeated this biasing 100 000 times and found that the probability to receive the final sample with the uncorrelated ($\rho < 0.15$) parameters z_0/h and B/T is 5×10^{-5}. This test proves that the lack of the correlation between the disc flatness and the bulge-to-total luminosity ratio cannot be caused by the fitting biases.

We also marked by squares early-type galaxies with *Type* ≤ 0 (Fig. 10, top plot). All these galaxies show a wide range of the ratio B/T from 0 to 0.8. They also demonstrate a significant scatter of z_0/h whereas the ratio z_0/h does not depend on B/T for these objects in accordance with the conclusion by Chudakova & Silchenko (2014). The dependence in Fig. 9 (top plot) is mainly created by these galaxies. The classification of these galaxies as S0 is expected to be biased because we cannot conclude the absence of a spiral structure in them. The number of galaxies classified as early-type galaxies in 2MASS and S^{4}G samples, in turn, is small. As a result, the dependence of z_0/h on *Type* for these samples is weak (Fig. 9, middle and bottom plots).

For both 2MASS and S^{4}G samples, we did not find any correlation between the flattening z_0/h and the ratio B/T as well. From the shown distribution, we can conclude again that the early-type galaxies may have stellar disc with different flatness, including very thin discs. The correlation between the relative thickness and the bulge contribution to the total luminosity is not confirmed for our samples.

4.3 The disc thickness versus the galaxy colour

One of the prominent correlations along the Hubble sequence is the morphological dependence on the integrated colour (see the review by Roberts & Haynes 1994). The early-type galaxies are mostly red whereas the late-type ones are mostly blue. Thus, the colour, in addition to the ratio B/T, is another indicator of the morphological type. The dispersion of the relation between the colour and the morphological type is large: there are some galaxies of Sc type which are red, and vice versa, there may be blue S0/a galaxies. As an example, among the sample of edge-on galaxies we found FGC 1597 (Scd) to be red and NGC 3600 (Sa) to be blue.

In fig. 7 from BKM14, there is no significant trend in the disc thickness with the overall galaxy colour $g - r$. In Fig. 11, we plot the z_0/h versus the $g - i$ for the SDSS sample (left-hand plot). The colours were corrected for the Milky Way reddening using the extinction maps by Schlegel, Finkbeiner & Davis (1998), but they were not corrected for the internal extinction in the galaxies.

Fig. 11 (left-hand plot) shows that there are two perpendicularly oriented clouds of galaxies. The bluer galaxies ($g - i \lesssim 1.0$) have stellar discs thinner ($z_0/h \approx 0.21 \pm 0.03$) than the red galaxies, which additionally reveal a wide scatter of the thickness ($z_0/h \approx 0.28 \pm 0.06$). It is well seen that there are red galaxies with both flat and thickened discs.

The latter can be interpreted in two ways. First, red galaxies (representing mostly early and intermediate types) can truly have thick or thin discs (as we could see in Fig. 1). Second, the dust lane (and the internal extinction in general) can cause the reddening. We tried to properly mask the dust lane while preparing the image for the decomposition. But remaining traces of the dust lane can alter the profile in the z-direction making it shallower. It results in a larger value of the z_0. In the latter case, the results of the decomposition should be biased, and the relative thickness z_0/h should be slightly overestimated. Almost all galaxies with the dust traces fall into the red cloud in the plot, while, as we can see, the dust-free galaxies fall into both clouds (Fig. 11, filled circles). Note that we cannot exclude biased decomposition in the i band even in the case of dust-free galaxies since we do not see the division into two clouds when using SDSS sample for the ratio B/T and *Type*. The galaxies with dust lanes sample the whole range of value B/T and *Type*. It indicates that the presence of the dust lanes marginally correlates with the B/T and *Type* (see, for example, Draine et al. 2007).

For both 2MASS and S^{4}G samples, there is no correlation between the disc thickness and the overall galaxy colour $B - I$ (middle and right plots). We can see only a slightly larger scatter for the ratio z_0/h in the redder side of the plot for the 2MASS sample.

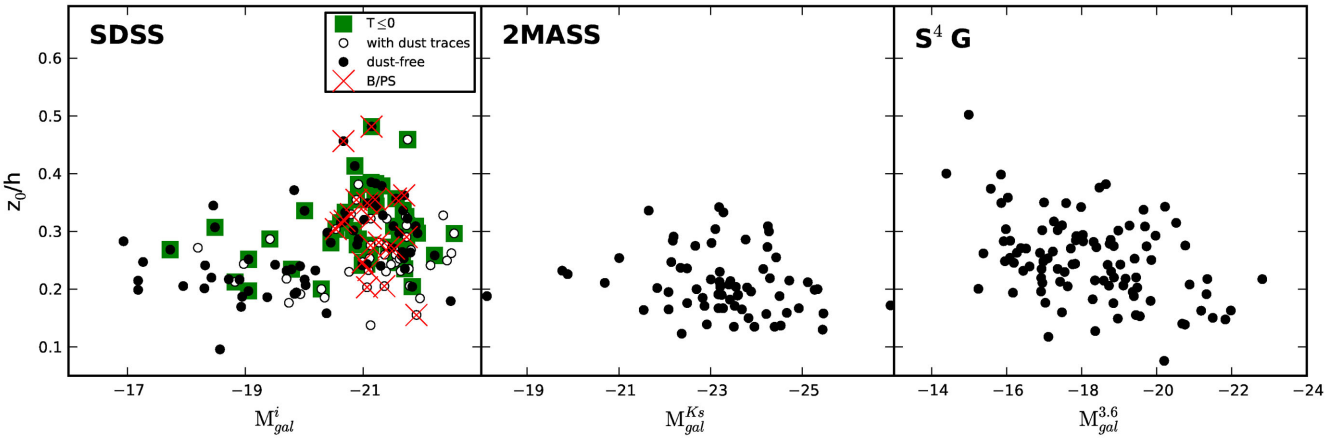

Figure 12. The dependence of the disc relative thickness on the total luminosity for the SDSS (*i* band), 2MASS (K_s band), and S^{4}G (3.6 μm) samples. The designation is kept the same as in Fig. 10.

Thus, the difference between the distributions of the parameters estimated from the optical SDSS and IR samples on the z_0/h–*colour* diagram may be interpreted by the presence of the dust component that affects the model decomposition. We suppose that even our 'dust-free' galaxies are not absolutely transparent in the *i* band, which biases the z_0/h estimation. However, this issue should be considered more carefully.

Another possible factor that biases interpretations of the plots is that the S^{4}G sample is deficient in early-type red galaxies and comprises a large fraction of blue galaxies. This fact can be one of the reasons why we do not see any subdivision of galaxies in the z_0/h–$B-I$ space for the S^{4}G sample.

4.4 The disc thickness versus galactic luminosity

We also analyse the dependence of the relative thickness z_0/h on the total luminosity of galaxies and find this correlation is weak if at all existing (see Fig. 12). Our SDSS sample demonstrates a large scatter for the ratio z_0/h in the bright side of the plot (Fig. 12, left-hand panel), which is similar to the presence of two perpendicular clouds in the z_0/h–$g-i$ diagram (see previous section). This scatter is mainly due to the presence of early-type galaxies (*Type* ≤ 0, squares in the plot), which show a large scatter of the ratio z_0/h.

It is well established that the dust content correlates well with the galaxy mass (e.g. Masters et al. 2010; Skibba et al. 2011), and we see that the bright region is populated mainly by the galaxies with dust traces.

Only one sample (S^{4}G) shows a hint of the thickness–luminosity relation: more luminous galaxies are thinner, on average. de Grijs (1998) also did not find any evidence for a dependence between the relative thickness and the absolute magnitude (see fig. 7b in de Grijs 1998). He referred to the theoretical prediction that the ratio h/z_0 should decrease rapidly from faint galaxies to a constant level for normal and bright galaxies (Bottema 1993) and claimed that it could not be confirmed observationally in his sample. Our samples also do not confirm this trend. Moreover, S^{4}G sample shows the inverse trend probably because of the large number of late-type (irregular) galaxies. However, this trend is consistent with the issue of the thickening of disc towards low mass reported in recent years in the literature (Sánchez-Janssen, Méndez-Abreu & Aguerri 2010; Roychowdhury et al. 2013).

5 DISCUSSION

5.1 The difference between the 1D and 2D decomposition results

The dependence of the stellar disc relative thickness on the *Type* reveals itself clearly only in the 1D modelling (de Grijs 1998; BKM14). This statement is also applicable to the dependence between the disc flatness z_0/h and the bulge-to-total luminosity ratio B/T. Fig. 13 demonstrates this dependence for the SDSS sample in the case of 1D analysis. The correlation between the disc thickness and B/T is good (the Pearson's correlation coefficient $\rho = 0.75$) for the subsample of 141 galaxies (black circles), and it is fairly good for the whole EGIS catalogue (grey dots, $\rho = 0.53$). However, the correlation does not appear at all if the 2D analysis results are used (see Fig. 10, top panel).

The correlation between the z_0/h and B/T parameters for the 1D analysis of the SDSS subsample galaxies can be explained by biased estimation of the disc structural parameters for the galaxies with significant bulge contribution. This is rather expected because in the early-type galaxies the extension of the bulge structure is much larger than that in late-type galaxies. The disc scaleheight z_0

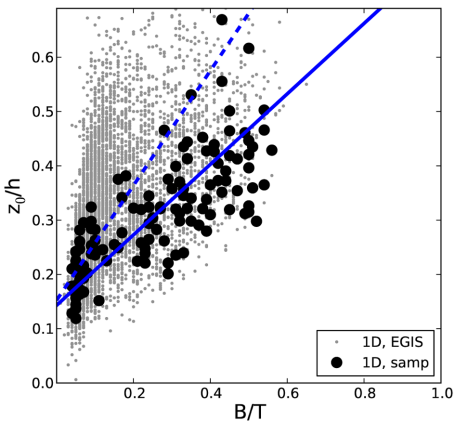

Figure 13. The distribution of the disc flatness as a function of the bulge-to-total luminosity ratio for the whole EGIS sample (grey dots) and for the subsample of 141 galaxies (black circles) estimated using the 1D decomposition in the *i* band. The dashed regression line is referred to the whole sample; the solid regression line is referred to the subsample.

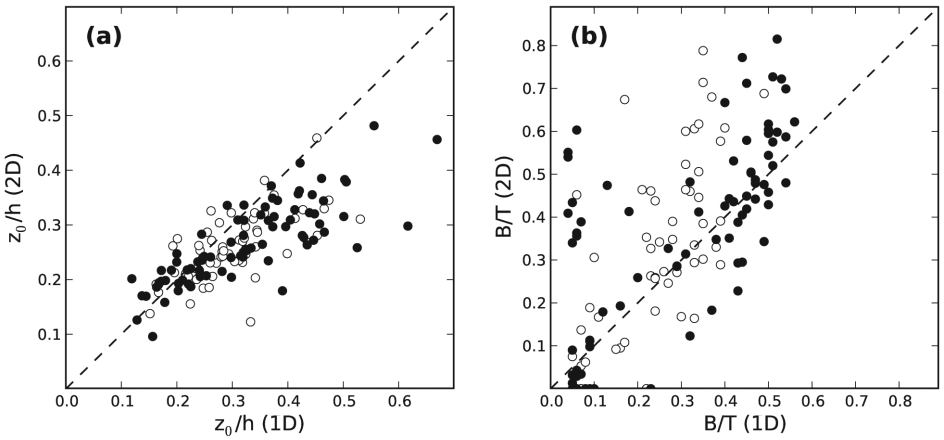

Figure 14. The comparison of the results for the z_0/h and B/T approximation between the 1D and 2D decomposition techniques. The open circles refer to the subsample of galaxies with slightly visible dust lanes; the filled circles refer to the reference subsample of galaxies without dust lanes.

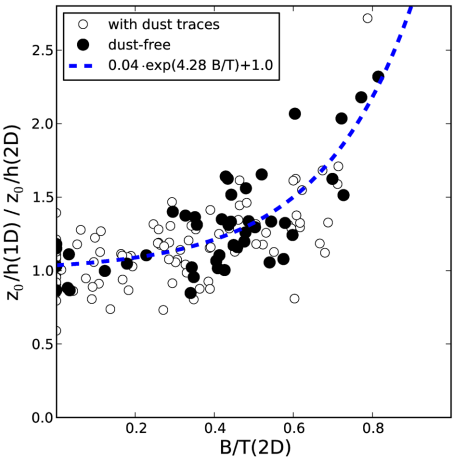

Figure 15. The dependence of the ratio of the stellar thicknesses in the 1D and 2D modelling versus the bulge-to-total luminosity ratio from the 2D analysis for our SDSS sample, *i* band. The open circles refer to the subsample of galaxies with slightly visible dust lanes; the filled circles refer to the reference subsample of galaxies without dust lanes. The dashed line is a simple exponential approximation to the data.

should be overestimated while analysing the vertical photometric disc profiles contaminated by the bulge light. At the same time, the radial scalelength should be underestimated. As a result, the ratio z_0/h will be overestimated in the early-type galaxies. The biased 1D decomposition leads also to the underestimation of the ratio B/T in comparison with 2D decomposition. In Fig. 14, we compare the results for the z_0/h and B/T approximation between the 1D and 2D decomposition techniques applied to our SDSS sample. The ratio z_0/h is overestimated for the 1D decomposition in comparison with the 2D decomposition (left-hand panel).

The biased decomposition in the 1D analysis reveals itself in the biased distribution of the ratio B/T (Figs 13 and 14, right-hand panel) in the comparison with the distribution over B/T in the 2D analysis (B/T < 0.6 for the 1D decomposition, and B/T spreads up to 0.8 for the 2D decomposition for the same galaxies). In the 1D analysis, the contribution of the bulge seems to be underestimated and the rest of the true bulge light (non-retrieved from the profile) contributes to the disc thickness.

In Fig. 15, the ratio of the stellar disc thickness in the 1D and 2D analysis versus the bulge-to-total luminosity ratio (from the 2D analysis) is shown. It is well seen that with the increasing of the B/T the relative thickness is growing with respect to the 2D approach (both for the whole sample and the reference subsample of 46 dust-free galaxies). In other words, the correlation in Fig. 13 may be a consequence of the biased model fitting in the 1D analysis, which dramatically affects the decomposition results for galaxies with significant non-disc components. A simple exponential approximation of data is shown in Fig. 15 by dashed line. We can see that for galaxies with B/T $\gtrsim 0.4$ the 1D disc flattening will overestimate more than 10 per cent the flattening found with the 2D method and more than twice for galaxies with B/T ≈ 0.8.

We summarize that the 1D and 2D methods produce different results as we can see by comparing Figs 13 and 10 (top panel). We assume that this difference is caused by biased estimation of the bulge contribution to the total luminosity in the 1D approach. With the 1D analysis, the bulge was not fitted at all and only its fraction was estimated which may bring wrong decomposition results for bulge-dominated galaxies. The 2D approach is a more robust method, which should report reliable results. The 3D analysis performed in BKM14 seems to be rather ambiguous, and it should be properly improved. Therefore, we do not discuss the results of this method here.

5.2 Morphological type estimation

The morphological classification of edge-on galaxies is a difficult task because of several aspects. First, the most essential criterion of the Hubble type, the tightness of the spiral pattern, cannot be applied to galaxies viewed edge-on. Second, dust attenuation dims the bulge in optics and NIR and hence, we are not able to estimate by eye the contribution of the bulge to the total luminosity in the galaxy reliably. Third, some structural details in a galaxy can be identified only via the inspection of its non-edge-on surface brightness maps. For instance, steps ('shoulders') at the photometric profile along the major axis of an edge-on galaxy can be an evidence of a bar or a ring, but they can also reveal the deviation of the disc surface brightness profile from the single exponent. Wrong morphological classification has been found for many galaxies when detailed bulge/disc decomposition was performed (see, for example, de Souza et al. 2004).

In order to demonstrate how the inclination of a galaxy can affect its morphological classification, we show the dependence between the B/T and *Type* for two subsamples from the S^{4}G catalogue

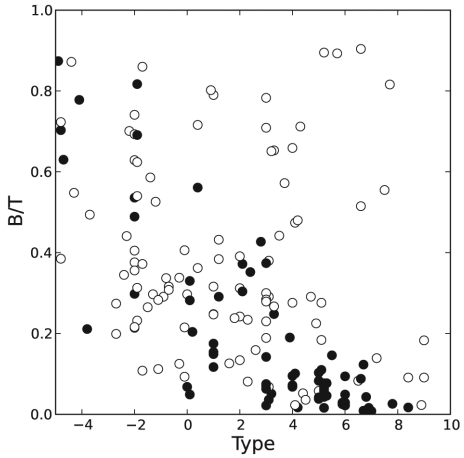

Figure 16. The distribution of the bulge-to-total luminosity ratio as a function of the morphological type for galaxies with inclination angles $i = 90^\circ$ (open circles) and $i < 30^\circ$ (black circles), in the S^{4}G sample (3.6 μm).

(Fig. 16). The first group contains galaxies with $i < 30^\circ$ (black circles). The second one comprises galaxies with $i = 90^\circ$ (open circles). Here, the inclination angle i is taken from the HyperLeda data base. Although some of these galaxies are not viewed perfectly edge-on, they are certainly highly inclined. In Fig. 16, one can see that the open circles have larger scatter, with many outliers in the right upper corner. This indicates that the morphological classification of edge-on galaxies is rather ambiguous. Observable strong dust attenuation can dim the bulge and hence bias the morphology classification for such objects towards the later types.

5.3 The model dependence of the obtained results

We should now make some comments on decomposing multicomponent galaxies. It is obviously difficult to unambiguously identify the presence of a bar in nearly edge-on systems. However, about half of disc galaxies demonstrates boxy/peanut-shaped structures in the central region (Lütticke, Dettmar & Pohlen 2000; Laurikainen et al. 2011), which is tagged by some authors as projection of the vertical structure of bars (Bureau & Freeman 1999; Chung & Bureau 2004).

It is apparent that for such galaxies the simple 'bulge+disc' model will not provide appropriate fitting. In this case, a 'bulge+disc+bar' modelling should be used instead. The bulge-to-total luminosity ratio and the relative disc thickness are expected to decrease in the case of the bar contribution. More detailed images of nearby galaxies show some other hidden features. For instance, the photometric decomposition of the Sombrero galaxy NGC 4594 revealed a disc, a bulge, an outer spheroid, a stellar ring, and a stellar, inner ring, or disc (Gadotti & Sánchez-Janssen 2012). However, in the case of such multicomponent structure the fitted model becomes ambiguous and suffers from the local χ^2 minimum degeneracy.

Also, some authors tried to find the parameters of thin and thick discs using a two-component model of the stellar disc (see, e.g., Yoachim & Dalcanton 2006; Comerón et al. 2011). In this work, we only studied one-component disc decompositions (mainly because of the shallow photometric depth of the surveys we work with and a lack of sufficient spatial resolution) following the works by de Grijs (1998) and Kregel et al. (2002). Studying larger samples in different photometrical bands, we did not find a correlation between the disc flattening and the morphological type, as well as between the disc flattening and the bulge contribution to the total galaxy luminosity.

Our next step in studying edge-on galaxies is building the best models of nearby, well-resolved edge-on galaxies using their multiband imaging, with proper dust-component treatment (see, e.g., Baes et al. 2011).

6 CONCLUSIONS

The results of our analysis of edge-on galaxies can be summarized as follows:

(i) In the course of our analysis, we obtained a counter-intuitive result – the disc relative thickness does not depend on the bulge-to-total luminosity ratio for all the samples studied. However, it may depend on the total luminosity in the near- and mid-infrared bands, in which the old stellar population contributes mainly in the disc luminosity, and reflects the dependence on the total mass (Sánchez-Janssen et al. 2010; Roychowdhury et al. 2013). The existence of the correlation between the disc flatness and the morphological type is only confirmed for the SDSS sample and late-type galaxies from the S^{4}G sample (anticorrelation).

These findings may have far-reaching consequences. Thus, since the relative thickness of the disc depends on the contribution of the spherical component ('bulge+dark halo') ($h/z_0 \propto M_{\rm dark}/M_{\rm total}$; Zasov, Makarov & Mikhailova 1991; Zasov et al. 2002, see also the discussion in MSR10 and Mosenkov, Sotnikova & Reshetnikov 2014), this means that the relative contribution of the spherical component does not vary systematically along the morphological Hubble sequence of bright spiral galaxies. In turn, since bulges contribute more to the mass of the spherical component in the early-type disc galaxies, the dark haloes themselves should reveal higher mass fraction in the case of the late-type (mostly bulgeless) galaxies.

At the same time, a compact but massive bulge stops the disc heating in the vertical direction due to the bending instability (Sotnikova & Rodionov 2006) and leaves the disc rather thin. In galaxies with large B/T ratio, we may expect observing stellar discs of either thickness. In Fig. 10, we see a large scatter of the ratio z_0/h for the galaxies with B/T > 0.4.

(ii) We conclude that the correlation between the morphological type and the disc flatness reported earlier by some authors (e.g. de Grijs 1998) was due to biased estimates of the disc flatness during the 1D analysis. Reanalysing the same data by the 2D method, Kregel et al. (2002) found the disc scaleheight to be overestimated for almost all galaxies studied with the 1D decomposition (see their fig. 2, bottom panel). At the same time, the disc scalelength was underestimated (the same fig. 2, top panel). As a result the relative thickness increases in the 1D analysis. We obtained the same result and extended it: the 1D decomposition overestimates the disc thickness mainly in the galaxies with large bulges (more than 10 per cent for galaxies with B/T $\gtrsim 0.4$), i.e. in all early-type disc galaxies. It is important to note that Kregel et al. (2002) did not present the correlation between the disc thickness and the galaxy type for the updated analysis. It was done by Hernandez & Cervantes-Sodi (2006) and is shown in their fig. 7. A glance at the plot suggests that the reported trend is poor and maintained by only one point representing a Sa type galaxy. Moreover, there are no galaxies earlier than the Sa in the sample by Kregel et al. (2002).

(iii) We also demonstrate that there is no correlation between the disc relative thickness and the galaxy colour. This fact strengthens our conclusion that there is no correlation between the thickness of the disc and the morphological type of the galaxy.

ACKNOWLEDGEMENTS

The authors express gratitude for the grant of the Russian Foundation for Basic Researches number 14-02-00810 and 14-22-03006-ofi. This work was partly supported by St Petersburg State University research grant 6.38.669.2013. AM is a beneficiary of a mobility grant from the Belgian Federal Science Policy Office. DB was partly supported by RSF via grant RSCF-14-22-00041.

We are thankful to the referee for his constructive comments which helped improve the quality and the presentation of the paper.

Funding for the SDSS has been provided by the Alfred P. Sloan Foundation, the Participating Institutions, the National Science Foundation, the US Department of Energy, the National Aeronautics and Space Administration, the Japanese Monbukagakusho, the Max Planck Society, and the Higher Education Funding Council for England. The SDSS Web Site is http://www.sdss.org/.

This research makes use of the NED which is operated by the Jet Propulsion Laboratory, California Institute of Technology, under contract with the National Aeronautics and Space Administration, and the LEDA data base (http://leda.univ-lyon1.fr). We also acknowledge the data products from the S^4G survey (http://www.cv.nrao.edu/∼ksheth/S4G/Site/S4G_Home.html) and the 2MASS, which is a joint project of the University of Massachusetts and the Infrared Processing and Analysis Center/California Institute of Technology, funded by the National Aeronautics and Space Administration and the National Science Foundation.

REFERENCES

Ahn C. et al., 2012, ApJS, 203, 21
Aihara H. et al., 2011, ApJS, 193, 29
Baes M. et al., 2010, A&A, 518, L39
Baes M., Verstappen J., De Looze I., Fritz J., Saftly W., Vidal Perez E., Stalevski M., Valcke S., 2011, ApJS, 196, 22
Bianchi S., 2007, A&A, 471, 765
Bizyaev D., Kajsin S., 2004, ApJ, 613, 886
Bizyaev D., Mitronova S., 2002, A&A, 389, 795
Bizyaev D. V., Kautsch S. J., Mosenkov A. V., Reshetnikov V. P., Sotnikova N. Ya., Yablokova N. V., Hillyer R. W., 2014, ApJ, 787, 24 (BKM14)
Bottema R., 1993, A&A, 275, 16
Bureau M., Freeman K. C., 1999, AJ, 118, 126
Bureau M., Aaronica G., Athanassoula E., Dettmar R. J., Bosma A., Freeman K. C., 2006, MNRAS, 370, 753
Busch G. et al., 2014, A&A, 561, A140
Chudakova E. M., Silchenko O. K., 2014, Astron. Rep., 58, 281
Chung A., Bureau M., 2004, AJ, 127, 3192
Comerón S. et al., 2011, ApJ, 741, 28
de Grijs R., 1998, MNRAS, 299, 595
de Jong R. S., 1996, A&A, 313, 45
De Looze I. et al., 2012, MNRAS, 427, 2797
de Souza R. E., Gadotti D. A., dos Anjos S., 2004, ApJS, 153, 411
Draine B. T. et al., 2007, ApJ, 663, 866
Erwin P., 2015, ApJ, 799, 226
Gadotti D. A., 2009, MNRAS, 393, 1531
Gadotti D. A., Sánchez-Janssen R., 2012, MNRAS, 423, 877
Guthrie B. N. G., 1992, A&AS, 93, 255
Häussler B., McIntosh D. H., Barden M., 2007, ApJS, 172, 615
Häussler B. et al., 2013, MNRAS, 430, 330
Hernandez X., Cervantes-Sodi B., 2006, MNRAS, 368, 351
Karachentsev I. D., Karachentseva V. E., Parnovsky S. L., 1993, Astron. Nachr., 313, 97
Karachentsev I. D., Karachentseva V. E., Kudrya Yu . N., Parnovsky S. L., 1997, Astron. Lett., 23, 573
Karachentsev I. D., Karachentseva V. E., Kudrya Yu . N., Sharina M. E., Parnovskij S. L., 1999, Bull. Spec. Astrophys. Obs., 47, 185
Kim T. et al., 2014, ApJ, 782, 64
Kregel M., van der Kruit P. C., de Grijs R., 2002, MNRAS, 334, 646
Laurikainen E., Salo H., Buta R., Knapen J. H., 2011, MNRAS, 418, 1452
Lütticke R., Dettmar R.-J., Pohlen M., 2000, A&AS, 145, 405
Ma J., Peng Q. H., Chen R., Ji Z. H., Tu C. P., 1997, A&AS, 126, 503
Ma J., Peng Q. H., Gu Q. Sh., 1998, A&AS, 130, 449
Ma J., Zhao J. L., Shu C. G., Peng Q. H., 1999, A&A, 350, 31
Masters K. L. et al., 2010, MNRAS, 404, 792
Mitronova S. N., Karachentsev I. D., Karachentseva V. E., Jarrett T. H., Kudrya Yu . N., 2003, Bull. Spec Astrophys. Obs., 57, 5
Mosenkov A. V., 2014, Astrophys. Bull., 69, 99
Mosenkov A. V., Sotnikova N. Ya., Reshetnikov V. P., 2010, MNRAS, 401, 559 (MSR10)
Mosenkov A. V., Sotnikova N. Ya., Reshetnikov V. P., 2014, MNRAS, 441, 1066
Naim A. et al., 1995, MNRAS, 274, 1107
Nair P. B., Abraham R. G., 2010, ApJS, 186, 427
Nilson P., 1973, Uppsala General Catalogue of galaxies. Acta Universitatis Upsalienis, Nova Regiae Societatis Upsaliensis, Series v: a Vol. 1
Paturel G., Petit C., Prugniel P., Theureau G., Rousseau J., Brouty M., Dubois P., Cambrésy L., 2003, A&A, 412, 45
Peng Q. H., 1988, A&A, 206, 18
Peng C. Y., Ho L. C., Impey C. D., Hans-Walter R., 2002, AJ, 124, 266
Peng C. Y., Ho L. C., Impey C. D., Hans-Walter R., 2010, AJ, 139, 2097
Roberts M. S., Haynes M. P., 1994, ARA&A, 32, 115
Roychowdhury S., Chengalur J. N., Karachentsev I. D., Kaisina E. I., 2013, MNRAS, 436, L104
Sánchez-Janssen R., Méndez-Abreu J., Aguerri J. A. L., 2010, MNRAS, 406, L65
Schlegel D. J., Finkbeiner D. P., Davis M., 1998, ApJ, 500, 525
Sérsic J. L., 1968, Atlas de Galaxias Australes. Observatorio Astronomico, Cordoba
Sheth K. et al., 2010, PASP, 122, 1397
Simard L. et al., 2002, ApJS, 142, 1
Skibba R. A. et al., 2011, ApJ, 738, 89
Skrutskie M. F. et al., 2006, AJ, 131, 1163
Sotnikova N.Ya., Rodionov S. A., 2006, Astron. Lett., 32, 649
Spitzer L., 1942, ApJ, 95, 325
Thuan T. X., Seitzer P. O., 1979, ApJ, 231, 680
van den Bergh S., 1998, Galaxy Morphology and Classification. Cambridge Univ. Press, Cambridge
van der Kruit P. C., Searle L., 1981a, A&A, 95, 105
van der Kruit P. C., Searle L., 1981b, A&A, 95, 116
van der Kruit P. C., Searle L., 1982a, A&A, 110, 61
van der Kruit P. C., Searle L., 1982b, A&A, 110, 79
Whaley C. H., Irwin J. A., Madden S. C., Galliano F., Bendo G. J., 2009, MNRAS, 395, 97
Xilouris E. M., Byun Y. I., Kylafis N. D., Paleologou E. V., Papamastorakis J., 1999, A&A, 344, 868
Yoachim P., Dalcanton J. J., 2006, AJ, 131, 226
Zasov A. V., Makarov D. I., Mikhailova E. A., 1991, Astron. Lett., 17, 374
Zasov A. V., Bizyaev D. V., Makarov D. I., Tyurina N. V., 2002, Astron. Lett., 28, 527

APPENDIX A: THE ESTIMATION OF THE GALAXY INCLINATION

In this work, we use two different approaches to estimate nearly edge-on galaxy disc inclination which are presented in detail by Mosenkov (2015, in preparation).

(1) The first approach is by using the *ExponentialDisk3D* function in the IMFIT code (Erwin 2015). The code has an advantage over GALFIT as it includes several 3D functions and the line-of-sight integration through a 3D luminosity–density model to create a projected

2D image. These functions are numerically integrated in each image pixel. The decomposition via the 3D integration is much slower than the 2D edge-on disc surface brightness evaluation (1). To speed up computations, we mask the central, bulge-dominated part in galaxies and use the *ExponentialDisk3D* function in the IMFIT to fit the periphery of the galaxies where the disc dominates. We chose the radius of the masking circle to be a half of the radius of the galaxy, which appears to be sufficient even for early-type galaxies.

The model parameters in the *ExponentialDisk3D* function include the disc exponential scalelength h, the vertical scaleheight z_0, the central luminosity density $I(0,0) = I_0^{\rm edge-on}/2h$ and the inclination angle of the disc i. In order to find the initial estimates of the galactic disc parameters, we use the DECA code where the disc is described by equation (1). These estimates are assumed as the initial values for running IMFIT, in combination with the assumption of $i = 90^\circ$. The output of this code is the set of the disc structural parameters, including the estimated inclination angle i.

In order to verify how well this method can estimate the inclination angle i of the stellar disc, we performed the same simulations as in Section 2.2, in which instead of using equation (1) for describing the edge-on disc, we used the *ExponentialDisk3D* function with three different values of i: 80°, 85°, and 90°. Then we fitted these simulated images with the *ExponentialDisk3D* function of IMFIT, where the initial disc parameters were estimated with the DECA code, and the central region with the bulge was masked. The results of the inclination angle estimation using IMFIT (the median value $\langle i \rangle$ and the standard deviation Δi) are compared with a priori known angles i:

$$i = 80^\circ : \langle i \rangle = 81\overset{\circ}{.}6,\ \Delta i = 3\overset{\circ}{.}6\,,$$

$$i = 85^\circ : \langle i \rangle = 85\overset{\circ}{.}4,\ \Delta i = 2\overset{\circ}{.}5\,,$$

$$i = 90^\circ : \langle i \rangle = 88\overset{\circ}{.}9,\ \Delta i = 1\overset{\circ}{.}8\,.$$

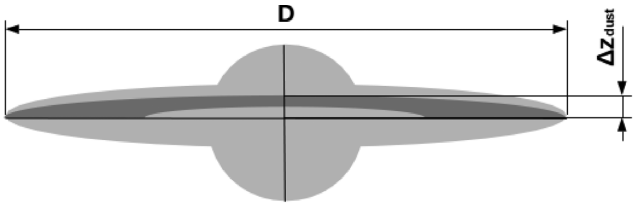

Figure A1. A sketch of a nearly edge-on galaxy with the dust lane (see the text).

The above results prove that this method can be used to estimate the inclination angle in the disc galaxies without dust attenuation and/or in the near- and mid-infrared bands. We found that masking of the bulge essentially reduces the computational time while has no strong effect on the results of the disc decomposition.

(2) The second method can be applied to the galaxies with visible dust lanes or with slight dust traces (similar to Bizyaev & Kajsin 2004). We make a natural assumption that the mid-planes of the stellar and dust discs coincide in the galaxies. We analyse 1D vertical photometric profiles cut along the minor axis and fit them with the Sérsic function. The deficiency of light found by comparing the model and the observing profiles, and the asymmetry of the profile relative to the centre of the galaxy indicate where the dust lane locates (its shift $\Delta z_{\rm dust}$ with respect to the galactic mid-plane). Knowing the diameter of the galaxy D and $\Delta z_{\rm dust}$, we can estimate the inclination angle of the galaxy i (see Fig. A1) as

$$i = \arccos\left(\frac{2\,\Delta z_{\rm dust}}{D}\right)\,. \qquad \text{(A1)}$$

This paper has been typeset from a TEX/LATEX file prepared by the author.